npj | precision oncology

Article

Published in partnership with The Hormel Institute, University of Minnesota

https://doi.org/10.1038/s41698-026-01523-w

Pan-cancer multi-omic integration of Trop2 reveals biological determinants and translational implications for ADC therapy

Giulia Notini[1,2,3,4,5,20], Barbara Galbardi[1,20], Giulia Viale[1,2,20], Matteo M. Naldini[1,2,6], Carlo Bosi[1,2,7], Giacomo De Micheli[2], Luca Licata[1,2], Marco Mariani[1,2,8], Marta Piras[9], Carmen Criscitiello[10,11], Marco Barreca[12,13], Maurizio Callari[13], Caterina Zanibelli[1,2], Francesca Patanè[1,2,11,14], Antonella Chiavassa[1,2,15], José Manuel Pérez-García[3,4,5], H. Raza Ali[6,16], Javier Córtes[3,4,5,17,18], Lajos Pusztai[8,19], Luca Gianni[13], Giampaolo Bianchini[1,2,21] ✉ & Matteo Dugo[1,21]

Trop2–directed antibody-drug conjugates (ADCs) show activity across epithelial cancers, yet determinants of target expression in tumors and normal tissues remain poorly defined. We integrated bulk and single-cell transcriptomic profiles from over 20,000 samples across TCGA, GTEx and public atlases to map TACSTD2 expression, regulation and functional correlates in solid malignancies and healthy epithelia. TACSTD2 was restricted to epithelial lineages, enriched in multiple tumors and detectable in selected normal epithelia. Genomic alterations were uncommon, whereas DNA methylation showed a consistent inverse association with expression, indicating dominant epigenetic control. TACSTD2 expression was linked to epithelial programs shaping the tumor microenvironment, including pathways related to barrier integrity and variable immune interactions across tumor types, with potential implications for combination with immune-checkpoint inhibitors. Across histologies, TACSTD2 showed modest and context-dependent co-expression with genes involved in ADC-processing and payload sensitivity. These findings indicate that antigen abundance alone is insufficient to predict ADC efficacy or toxicity across histologies.

Trophoblast cell surface antigen 2 (Trop2), encoded by the *TACSTD2* gene, is a 323 amino acids transmembrane glycoprotein that plays a pivotal role in various cellular processes[1], including calcium-signal transduction and cell proliferation[1–4].

Trop2 is broadly overexpressed in human malignancies[5], with the highest tumor-to-normal expression differences observed in cervical, head and neck, and bladder cancers[6].

While Trop2 is not sufficient to induce malignant transformation, its overexpression supports tumor growth[7]. Moreover, clinical trials identified Trop2 as a negative prognostic factor, correlating with shorter overall survival (OS) and progression-free survival (PFS) across multiple solid tumors[8]. Taken together, mechanistic and clinical observations identify Trop2 as a relevant therapeutic target.

[1]Medical Oncology Department, IRCCS San Raffaele Hospital, Milan, Italy. [2]Medicine and Surgery Department, Vita-Salute San Raffaele University, Milan, Italy. [3]International Breast Cancer Center (IBCC), Pangaea Oncology, Quiron Group, Barcelona, Spain. [4]Medica Scientia Innovation Research (MEDSIR), Barcelona, Spain. [5]Medica Scientia Innovation Research (MEDSIR), Cambridge, Massachusetts , USA. [6]CRUCK Cambridge Institute, University of Cambridge, Cambridge, UK. [7]Department of Radiation Oncology, New York-Presbyterian/Weill Cornell Medicine, New York, NY, USA. [8]Yale Cancer Center, New Haven, CT, USA. [9]Divisione di Senologia Medica, IEO – Istituto Europeo Oncologico, Milan, Italy. [10]IRCCS Humanitas Research Hospital, Milan, Italy. [11]Department of Biomedical Sciences, Humanitas University, Milan, Italy. [12]Department of Biotechnology and Biosciences, University of Milano-Bicocca, Milan, Italy. [13]Fondazione Michelangelo, Milan, Italy. [14]Medical Oncology Department, AOUP Santa Chiara, Pisa, Italy. [15]Department of Radiological, Oncological and Pathological Science, Sapienza University of Rome, Rome, Italy. [16]Department of Histopathology, Addenbrookes Hospital, Cambridge, UK. [17]IOB Madrid, Institute of Oncology, Hospital Beata María Ana, Madrid, Spain. [18]Department of Medicine, Faculty of Biomedical and Health Sciences, Universidad Europea de Madrid, Madrid, Spain. [19]Yale University, School of Medicine, New Haven, CT, USA. [20]These authors contributed equally: Giulia Notini, Barbara Galbardi, Giulia Viale.[21]These authors jointly supervised this work: Giampaolo Bianchini, Matteo Dugo. ✉e-mail: bianchini.giampaolo@hsr.it

THE HORMEL INSTITUTE
UNIVERSITY OF MINNESOTA

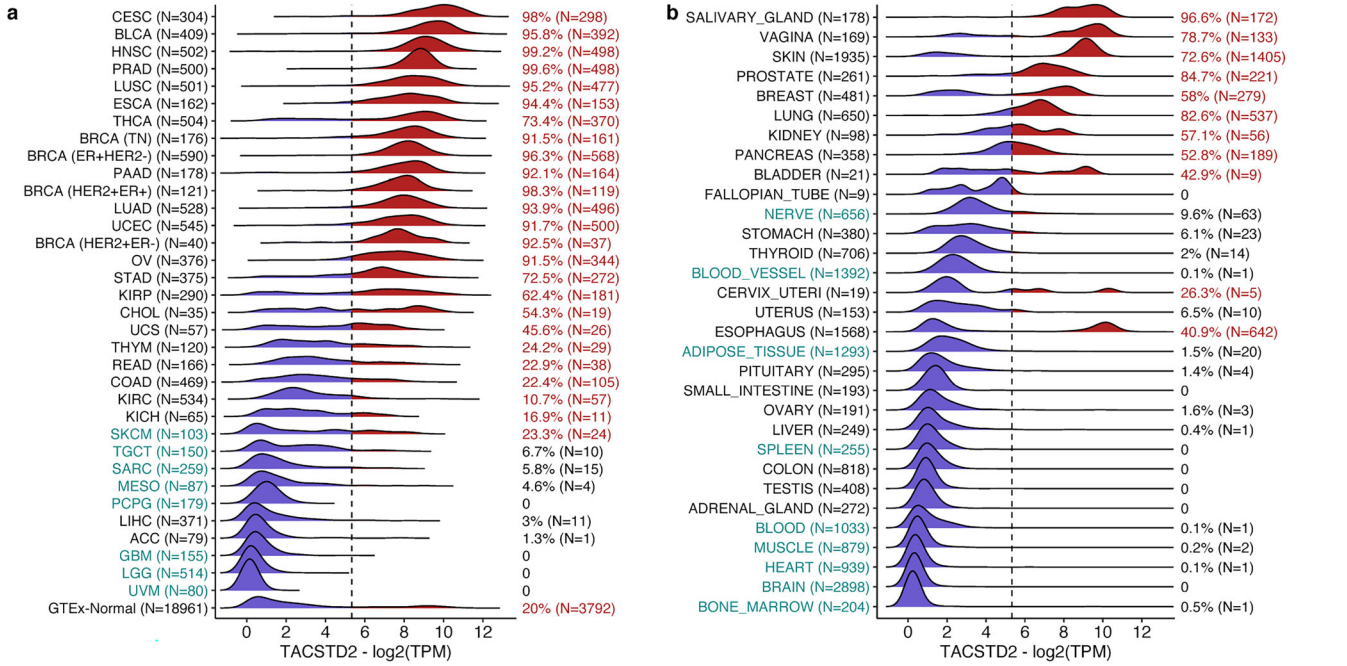

Fig. 1 | TACSTD2 expression in tumor and normal tissues. a Density plots showing the distribution of expression values of TACSTD2 in each cancer type, compared to normal tissues of GTEx. The vertical dashed line represents the 80th percentile of the TACSTD2 distribution in GTEx normal tissues. Expression values above this threshold are highlighted by red density curves. The percentage and number of samples above this threshold are reported on the right. Cancer types with more than 10% of samples with TACSTD2 expression above the selected threshold are highlighted in red. Non-epithelial cancer types are highlighted in green. **b** Density plots showing the distribution of expression values of TACSTD2 in GTEx normal tissues. The vertical dashed line represents the overall 80th percentile of the TACSTD2 distribution. Expression values above this threshold are highlighted by red density curves. The percentage and number of samples above this threshold are reported on the right. Tissues with more than 10% of samples with TACSTD2 expression above the selected threshold are highlighted in red. ACC adrenocortical carcinoma, BLCA bladder urothelial carcinoma, BRCA breast invasive carcinoma, CESC cervical squamous cell carcinoma, CHOL cholangiocarcinoma, COAD colon adenocarcinoma, ESCA esophageal carcinoma; GBM glioblastoma multiforme, HNSC head and neck squamous cell carcinoma, KICH kidney chromophobe, KIRC kidney renal clear cell carcinoma, KIRP kidney renal papillary cell carcinoma, LGG lower-grade glioma, LIHC liver hepatocellular carcinoma, LUAD lung adenocarcinoma, LUSC lung squamous cell carcinoma, OV ovarian serous cystadenocarcinoma, PAAD pancreatic adenocarcinoma, PRAD prostate adenocarcinoma, READ rectum adenocarcinoma, SARC sarcoma, SKCM skin cutaneous melanoma, STAD stomach adenocarcinoma, THCA thyroid carcinoma, UCEC uterine corpus endometrial carcinoma, UCS uterine carcinosarcoma, UVM uveal melanoma, TNBC triple-negative breast cancer, HER2 + HER2-positive breast cancer, HR + hormone receptor–positive breast cancer.

Antibody-drug conjugates (ADCs) have become a milestone of cancer therapy. ADCs consist of potent cytotoxic payloads linked to monoclonal antibodies, thereby creating a targeted delivery system that maximizes tumor uptake while reducing off-tumor toxicities.

Sacituzumab govitecan (SG), the first anti-Trop2 ADC, received accelerated FDA approval in 2020 for metastatic triple-negative breast cancer[9], later expanding to HR+/HER2-disease[10]. Its development paved the way for next-generation Trop2-targeting ADCs, such as datopotamab deruxtecan (Dato-DXd) and sacituzumab tirumotecan, which have shown promising activity across solid tumors, including breast and lung cancers.

Preclinical studies have identified target expression as a critical determinant of ADC efficacy, including anti-Trop2 agents[11–14]. However, data from clinical trials indicate that the relationship between target expression and response to ADC treatment is not consistently linear. In fact, in the TROPHY-U-01 study of metastatic urothelial cancer treated with SG, overall response rate (ORR) did not significantly differ across Trop2 expression levels[15]. Similar findings were reported in the TROPiCS-02 trial in metastatic breast cancer, where the efficacy of SG was comparable regardless of Trop2 expression levels[10]. Conversely, exploratory biomarker analyses from the ASCENT trial indicated that patients with high or medium Trop2 expression derived greater benefit from SG compared to those with low expression[16].

Importantly, assessment of Trop2 expression is not standardized. Some studies rely on immunohistochemistry (IHC), which requires standardized testing and is subject to significant interobserver variability among pathologists. Other studies evaluate mRNA expression. In addition, the variability in Trop2 expression over time[17], likely influenced by therapeutic selective pressure, and across different metastatic sites[18,19], adds another layer of complexity. Together, these factors may contribute to discrepancies between expression patterns and clinical outcomes observed across clinical trials.

To date, Trop2 expression levels in healthy tissues have not been associated with the incidence or severity of adverse events related to anti-Trop2 ADCs.

Arguably, sensitivity to a specific ADC is a multi-layered process influenced by target antigen density and heterogeneity, endocytic trafficking, lysosomal processing, linker stability/cleavage, cellular susceptibility, payload efflux, and modulators within the tumor microenvironment (TME)[6]. Although several genes have been individually linked to ADC efficacy in preclinical testing[6,20] and in clinical trials[16,21], an integrated framework explaining clinical efficacy, resistance, and adverse events is still lacking.

In this study, we investigated the molecular alterations and biological mechanisms associated with Trop2 expression in both healthy and solid tumor tissues using the publicly available GTEx[22] and TCGA pan-cancer[23] datasets. Our analyses suggest potential mechanisms underlying the efficacy

and toxicity of anti-Trop2 ADCs currently in advanced stages of development and generate hypotheses on potential therapeutic co-targets, thereby expanding the application of Trop2 targeting agents into additional tumor types.

Results

Trop2 expression across normal tissues and tumor types: insights from GTEx, TCGA and single-cell analyses

Pan-cancer analysis integrating GTEx (healthy tissue) and TCGA (tumor tissue) datasets revealed broad but heterogeneous *TACSTD2* expression across tissues (Fig. 1 and Figure S1).

Across tumor types, *TACSTD2* was consistently more expressed in cancers than in their normal counterparts. Using the 80th percentile of normal-tissue expression as a cut-off, 25 of 34 cancer types showed ≥10% "Trop2-high" samples (Fig. 1a).

High *TACSTD2* expression was observed in epithelial-derived cancers such as cervical (CESC, 98%), bladder (BLCA, 95.8%), lung (LUSC, 95.2%), pancreatic (PAAD, 92.7%), prostate (PRAD, 99.6%), and breast cancers, especially HER2-positive (98.4%) and TNBC (91.5%) subtypes. In contrast, tumor of non-epithelial origin, like sarcomas (SARC), gliomas (GBM and PCPG), and uveal melanomas (UVM), showed consistently low or absent expression, confirming the epithelial specificity of Trop2. Interestingly, certain tumor types like thyroid carcinoma (THCA), kidney renal papillary carcinoma (KIRP), cholangiocarcinoma (CHOL), and uterine carcinosarcoma (UCS) showed a wide range of expression, indicating a high inter-patient heterogeneity for *TACSTD2* expression (Figure S1). Overall, *TACSTD2* expression in tumors was not associated with age and sex (Figure S2). However, a physiological decline with aging was observed in the normal lung, pancreas, and prostate (FDR < 0.05).

Among normal tissues, epithelial-rich organs (salivary gland, vagina, skin) displayed the highest *TACSTD2* levels, whereas non-epithelial tissues (bone marrow, brain, muscle) showed minimal expression (Fig. 1b). For instance, salivary gland showed >90% *TACSTD2*-high samples, whereas brain and muscle showed <1%. Again, wide expression range with bimodal distribution was highlighted in certain normal tissues such as vagina, skin, breast, cervix uteri, and esophagus.

To overcome the limitations of bulk transcriptomic data, which represent an averaged signal from heterogeneous cell populations, single-cell RNA-Seq data from multiple tumor sites and normal tissues were analyzed to assess the intratumoral heterogeneity of *TACSTD2* expression and its cell-type specificity (Fig. 2a-c). The single-cell RNA-Seq analysis confirmed that *TACSTD2* expression is predominantly localized to malignant and normal epithelial cells. Across datasets, >70–95% of malignant epithelial cells showed detectable *TACSTD2* expression, whereas < 2% of stromal, immune or endothelial cells expressed the gene, consistent with observations from TCGA bulk tumor analyses (Fig. 2a). Single cell RNA-Seq data from normal tissues confirmed the epithelial origin of *TACSTD2* expression since tissues with high epithelial content like bronchus, tongue, endometrium, and salivary gland were among the highest expressors (Fig. 2b). Cell-type stratification showed the highest *TACSTD2* expression in basal respiratory cells, keratinocytes, squamous epithelia, and ductal cells (Fig. 2c). Stromal, immune, and fibroblast populations displayed negligible expression, consistent with the predominant localization of Trop2 to epithelial compartments.

TACSTD2 genetic and epigenetic alterations

Somatic mutations in the *TACSTD2* gene were infrequent across cancer types, occurring in a median of 0.3% of tumors (range 0-1.8%)(Figure S3a). Notably, all somatic mutations identified were private, each occurring in a single patient, with no evidence of clear hotspot mutational sites (Figure S3b). Similarly, copy-number amplifications were infrequent (< 5%) and deletions absent, supporting the stability of *TACSTD2* at the genomic level.

Given the minimal contribution of genomic variation, we next assessed epigenetic regulation through the methylation profile of the gene across different cancer types (Fig. 3). The 16 methylation sites covered by TCGA data along the *TACSTD2* gene body were highly correlated, with similar methylation levels in each sample (Fig. 3). Methylation levels varied significantly by tumor type. We observed an inverse correlation between TACSTD2 methylation and expression levels: cancers with high *TACSTD2* expression (e.g., CESC, BLCA, HNSC) showed strong hypomethylation, whereas LGG, UVM, and LIHC were hypermethylated and low-expressing. Correlation between CNAs and *TACSTD2* expression was overall poor, indicating that *TACSTD2* dysregulation in tumors may occur predominantly through epigenetic mechanisms rather than genomic alterations.

We next assessed whether *TACSTD2* expression was associated with genomic alterations of key oncogenes and tumor suppressors (Figure S4), hypothesizing that *TACSTD2* expression may be inferred by clinically relevant mutations that, unlike TACSTD2 expression assessment, are already routinely evaluated in diagnostic assessment of several tumor types. Moreover, recognizing tumor contexts in which high *TACSTD2* expression co-occurs with targetable oncogenic events may also help inform drug-development strategies, including the design of Trop2–directed ADCs with tailored payloads, rational combination approaches, and improved patient selection in both clinical and research settings.

We identified genes whose somatic mutational status was statistically significantly associated with *TACSTD2* expression. In thyroid carcinoma (THCA), tumors with *BRAF* mutations showed significantly higher *TACSTD2* levels, while those with *NRAS* mutations had reduced expression compared to wild-type samples. In pancreatic adenocarcinoma (PAAD), *KRAS* mutations were linked to higher *TACSTD2* expression in respect to their wild-type counterpart. Conversely, in thymoma (THYM), *HRAS* mutations were associated with increased expression (Figure S4).

Additionally, in lung adenocarcinoma (LUAD), *CDKN2A* deletions corresponded to increased *TACSTD2* expression compared to samples with normal *CDKN2A* status, while *CDKN2A* amplifications led to diminished TACSTD2 levels. Notably, *ERBB2* amplification in cervical squamous cell carcinoma (CESC) was significantly associated with overall reduced *TACSTD2* expression, while *ERBB2* amplification in stomach adenocarcinoma (STAD) was significantly correlated with higher *TACSTD2* expression (Figure S4).

Pan-cancer biological processes associated with Trop2-expression

To quantitatively investigate the relationship between *TACSTD2* expression and the tumor-immune microenvironment, we integrated immune deconvolution and pathway-level analyses across TCGA tumor types (Fig. 4). Immune and stromal cell populations were estimated using the consensusTME framework. Correlation analyses between *TACSTD2* expression and inferred cell-type abundances revealed marked heterogeneity across tumor types. In certain epithelial cancers, like kidney renal clear cell carcinoma (KIRC) and CHOL, *TACSTD2* expression was positively associated with stromal populations, including fibroblasts, while showing weak or negative correlations with cytotoxic immune cells, supporting a phenotype consistent with immune exclusion. In other tumor types, *TACSTD2* displayed poor or modest associations with immune infiltrates. In tumors like THCA and KICH *TACSTD2* was strongly associated with immune cell types infiltration.

To further characterize the biological functions, we performed single-sample gene set scoring for the MSigDB Hallmark gene sets. *TACSTD2* expression showed heterogeneous associations with immune-related pathways, including interferon-γ response and inflammatory signaling, without a consistent pan-cancer enrichment pattern.

Notably, *TACSTD2* expression was more consistently associated with epithelial and structural programs (e.g., apical surface and apical junction) than with immune activation signatures, reinforcing its role as a marker of epithelial differentiation rather than a direct indicator of immune engagement. No consistent association between TACSTD2 expression and proliferation signatures was observed.

Together, these findings indicate that *TACSTD2* expression does not uniformly define immune-inflamed or immune-desert phenotypes, but

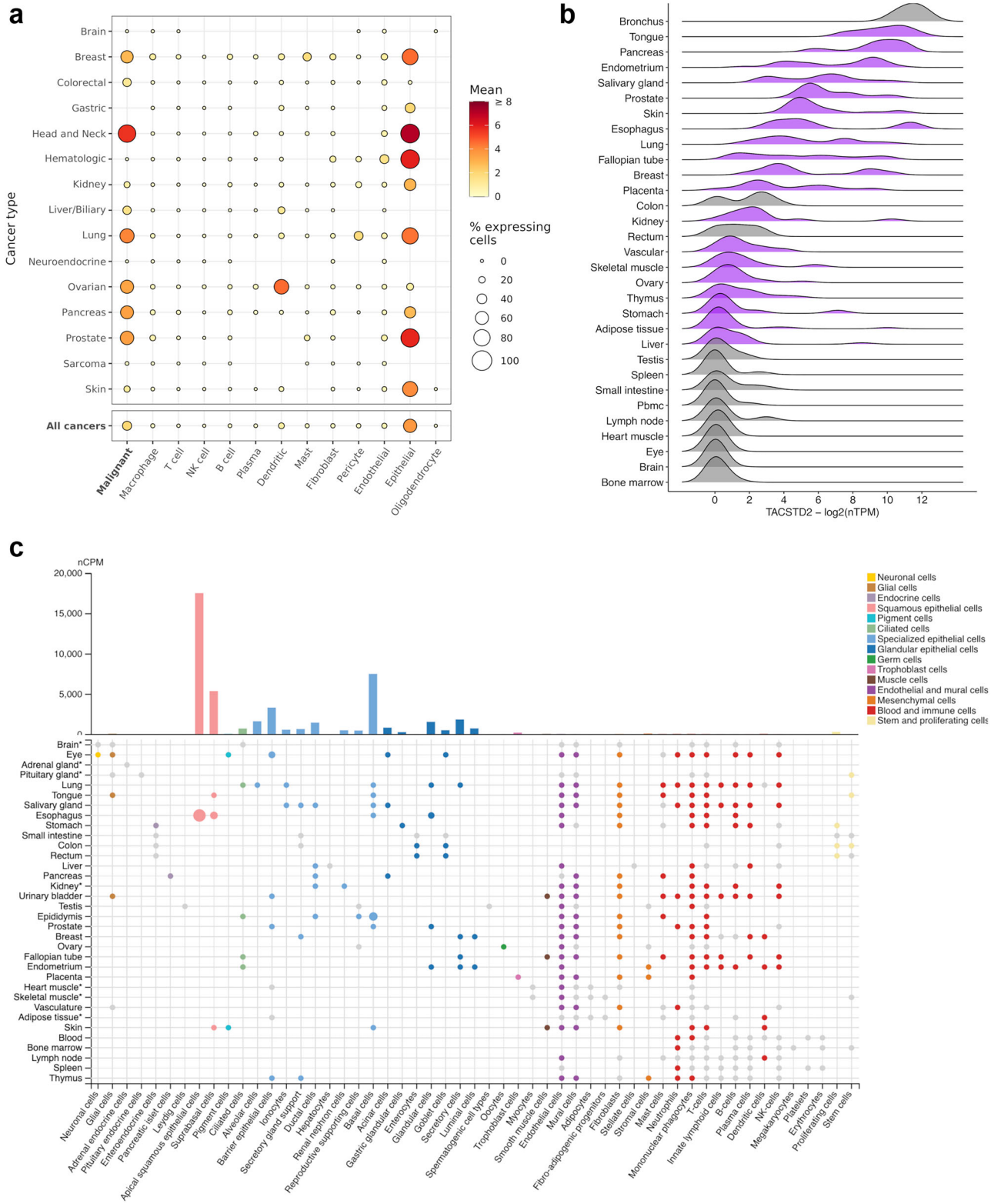

Fig. 2 | Single-cell expression of TACSTD2 in cancer and normal tissues. a Bubble plot showing the mean single-cell expression and % of expressing cells in multiple cancer types collected in the 3CA database. **b** Density plots showing the overall distribution of expression values of TACSTD2 in single cells from normal tissues of the Human Protein Atlas database. Data are shown as log2-normalized TPM. Tissues with an expression range ≥ 4 logs are highlighted in purple. **c** Normalized expression (nTPM) of TACSTD2 for each cell type in each tissue according to data obtained from the Human Protein Atlas. The size of the dot is proportional to the expression level. The bar plot on top shows the nTPM for each cell type.

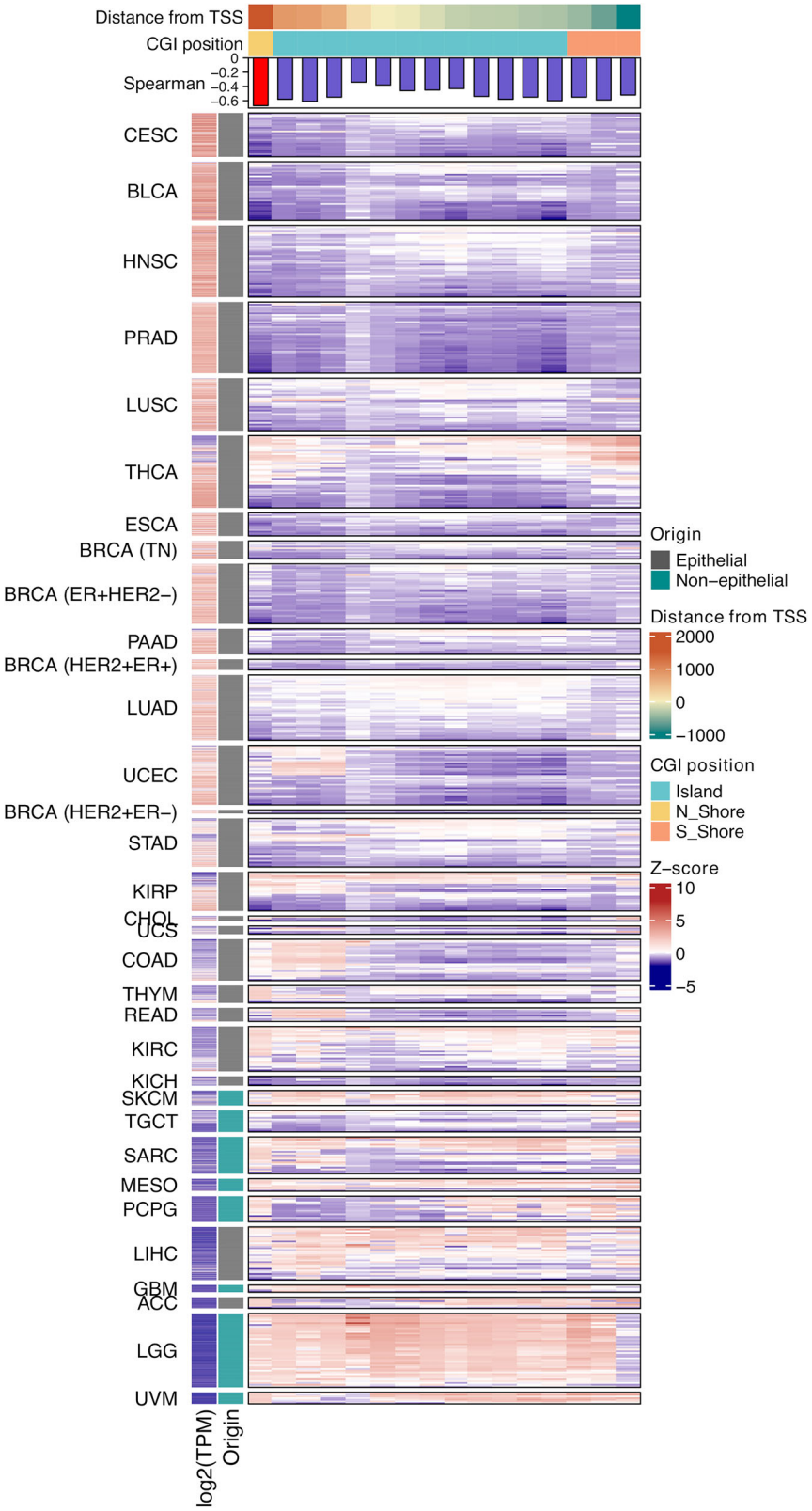

Fig. 3 | Correlation of TACSTD2 expression with CNAs and methylation. Heatmap showing absolute copy-number status (CNA) and standardized methylation beta values of probes targeting TACSTD2 gene. A higher beta value is an indication of higher methylation. Cancer types are ordered according to the median level of TACSTD2, as in Fig. 1 panel A. On top of the heatmap are shown the distance of the methylation probes from the transcription start site (TSS) and the CpG island positions. Spearman correlation of CNA and methylation with TACSTD2 expression is reported. ACC adrenocortical carcinoma, BLCA bladder urothelial carcinoma, BRCA breast invasive carcinoma, CESC cervical squamous cell carcinoma, CHOL cholangiocarcinoma, COAD colon adenocarcinoma, ER estrogen receptor, ESCA esophageal carcinoma, GBM glioblastoma multiforme, HER2 human epidermal growth factor receptor, HNSC head and neck squamous cell carcinoma, KICH kidney chromophobe, KIRC kidney renal clear cell carcinoma, KIRP kidney renal papillary cell carcinoma, LGG lower-grade glioma, LIHC liver hepatocellular carcinoma, LUAD lung adenocarcinoma, LUSC lung squamous cell carcinoma, OV ovarian serous cystadenocarcinoma, PAAD pancreatic adenocarcinoma, PRAD prostate adenocarcinoma, READ rectum adenocarcinoma, SARC sarcoma, SKCM skin cutaneous melanoma, STAD stomach adenocarcinoma, THCA thyroid carcinoma, TN triple-negative, UCEC uterine corpus endometrial carcinoma, UCS uterine carcinosarcoma, UVM uveal melanoma.

rather identifies epithelial programs that shape the tumor–immune interface in a tumor-type–specific manner.

We next performed a deeper investigation of the genes contributing to these enriched pathways. Several keratin genes, including *KRT14, KRT5, KRT16, KRT17*, and *KRT10*, demonstrated strong positive correlations with *TACSTD2* expression, consistent with its link to a basal/squamous gene expression program (Figure S5). Likewise, genes involved in cell–cell adhesion and epithelial integrity, such as *CLDN7* and *CLDN4*, were frequently co-expressed with *TACSTD2*. Moreover, genes associated with extracellular matrix remodeling and basement membrane adhesion, such as *ITGB4, LAMC2*, and *COL17A1*, were found to be upregulated in tumors with high *TACSTD2* expression.

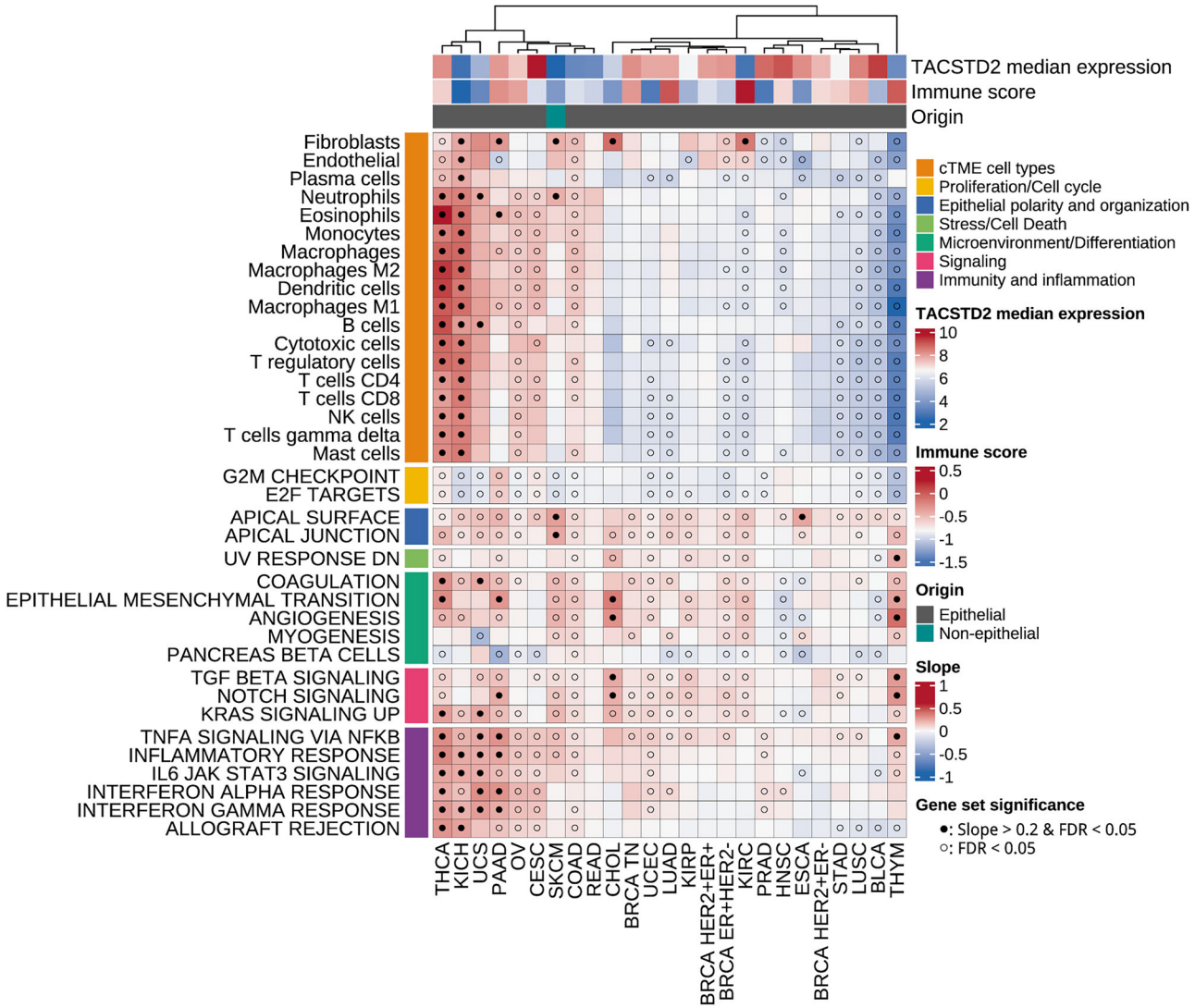

Fig. 4 | TACSTD2 association with biological pathways and immune cell types. Heatmap showing the beta coefficients of the linear model estimated between TACSTD2 expression and single-sample scores for cTME cell types and hallmark gene sets. The median expression of TACSTD2 in each cancer type is shown above. BLCA bladder urothelial carcinoma, BRCA breast invasive carcinoma, CESC cervical squamous cell carcinoma, CHOL cholangiocarcinoma, ER estrogen receptor, ESCA esophageal carcinoma, HER2 human epidermal growth factor receptor, HNSC head and neck squamous cell carcinoma, KICH kidney chromophobe, KIRC kidney renal clear cell carcinoma, KIRP kidney renal papillary cell carcinoma, LUAD lung adenocarcinoma, LUSC lung squamous cell carcinoma, OV ovarian serous cystadenocarcinoma, PAAD pancreatic adenocarcinoma, PRAD prostate adenocarcinoma, SKCM skin cutaneous melanoma, THCA thyroid carcinoma, TN triple-negative, UCS uterine carcinosarcoma.

Prognostic relevance of TACSTD2 expression across cancer types

To assess the prognostic relevance of *TACSTD2* expression, we performed survival analyses across TCGA tumor types, evaluating its association with overall survival (OS) and progression-free interval (PFI) using Cox-proportional hazards models (Figure S6a). Across the majority of histologies, *TACSTD2* expression was not significantly associated with either OS or PFI, consistent with its role as a marker of epithelial lineage rather than a universal driver of tumor aggressiveness. However, in pancreatic adenocarcinoma (PAAD), high *TACSTD2* expression was significantly associated with worse OS ($p = 0.024$) and shorter PFI ($p = 0.0072$), as confirmed by Kaplan-Meier analysis (Figure S6b). Conversely, in BRCA ER + HER2− and kidney renal papillary cell carcinoma (KIRP), high *TACSTD2* expression was associated with shorter PFI ($p = 0.013$ and $p = 0.0069$, respectively), while no significant association with OS was observed in these subtypes. No significant associations were detected in the remaining tumor types for either endpoint. Taken together, these findings indicate that the prognostic impact of *TACSTD2* expression is highly context-dependent, being most clinically relevant in PAAD, where it may reflect a more aggressive tumor phenotype.

Potential role of putative determinants of Anti-Trop2 ADC activity in predicting tumor response and toxicity

To investigate whether the activity of Trop2-directed ADCs might be modulated by genes involved in intracellular drug processing, we correlated the expression of *TACSTD2* and of key ADC-processing genes (*CTSB, CTSL*, and *TOP1*) which mediate linker cleavage and payload activation. Given their biological roles, expression of these genes in normal tissues could influence toxicity patterns, whereas expression in tumors might impact therapeutic efficacy. Across cancer types, correlations were modest and heterogeneous (median spearman: 0.11; range: −0.29–0.59), with positive associations in certain malignancies (e.g., *CTSB* in UCS) and negative in others (*CTSL* in HNSC, *TOP1* in READ/ESCA) (Figure S7).

To explore the potential clinical relevance of TACSTD2 and ADC-processing genes, we evaluated whether their expression might

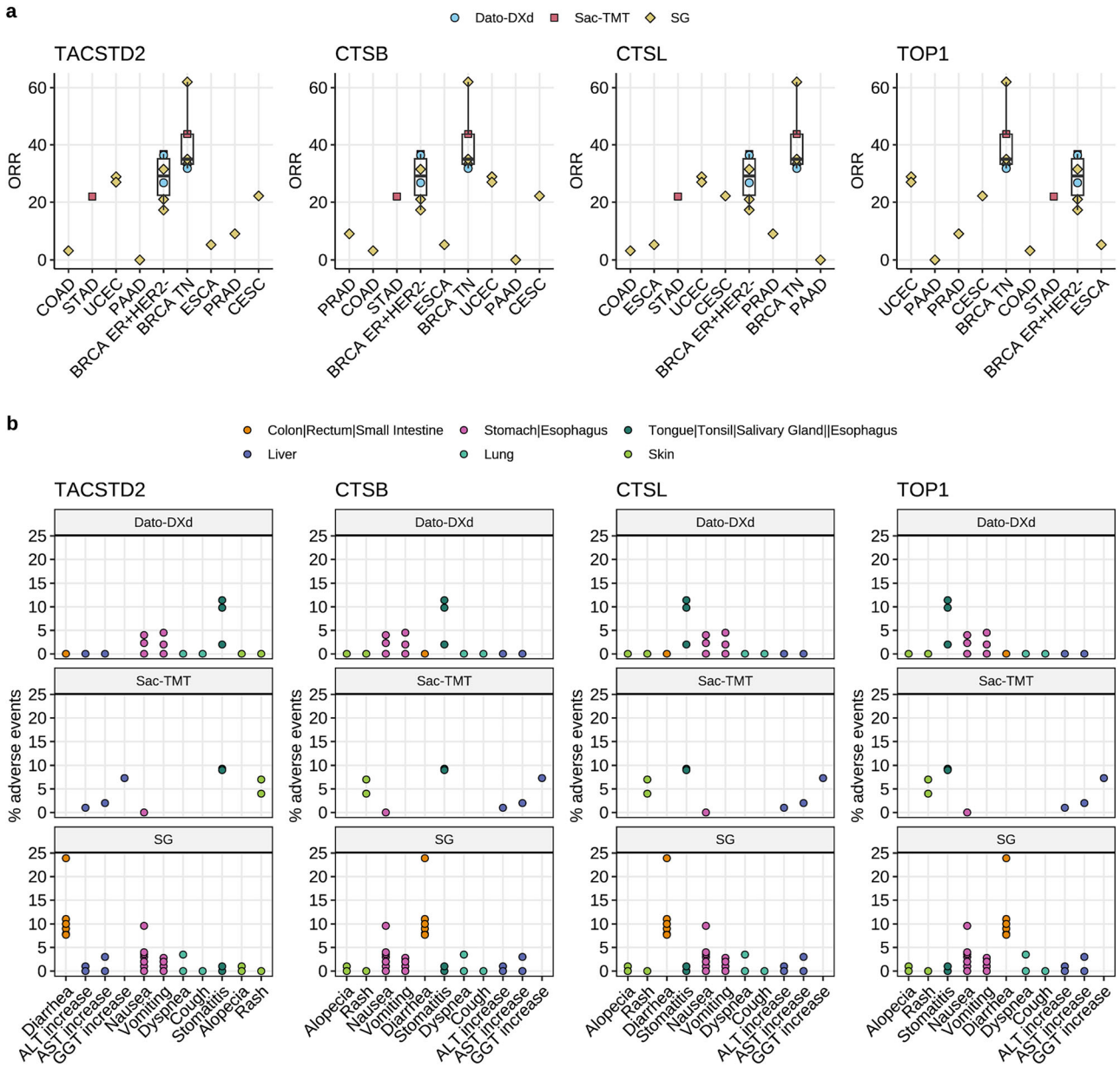

Fig. 5 | Link between gene expression, response, and adverse events in anti-Trop2 clinical trials. a Plot showing the median expression of TACSTD2, CTSB, CTSL, and TOP1 across TCGA tumor types (log2-TPM) plotted against objective response rates (ORRs) from monotherapy trials of anti–Trop2 ADCs. Cancer types are ranked from left to right according to the increasing median expression of the gene in TCGA. Each point represents the ORR results of each trial, and is placed above the tumor type in which the trial included patients with that disease. Points shapes and colors distinguish the three different anti-Trop2-ADCs as reported in the legend above. **b** Percentage of adverse events (AEs) reported in the same ADC trials, stratified by AE type. AEs on the x-axis are ranked from left to right according to the increasing median expression of TACTSD2 in the tissues associated with each AE. Point colors denote the organs associated with each AE, as reported in the legend above. Panels are organized by ADC (top: Dato-DXd; middle: Sac-TMT; bottom: SG). BRCA breast invasive carcinoma, CESC cervical squamous cell carcinoma, COAD colon adenocarcinoma, ER estrogen receptor, ESCA esophageal carcinoma, HER2 human epidermal growth factor receptor, PAADpancreatic adenocarcinoma, PRAD prostate adenocarcinoma, STAD stomach adenocarcinoma, TN triplenegative, UCEC uterine corpus endometrial carcinoma.

correlate with tumor sensitivity to anti-Trop2 ADC monotherapy. In the absence of transcriptomic data from clinical samples of patients enrolled in anti-Trop2 clinical trials, we performed an indirect comparison by ranking trial-reported objective response rates (ORRs) according to the median expression of these genes in TCGA (Fig. 5a). No clear linear association emerged. Tumor types such as triple-negative and hormone receptor–positive breast cancers, characterized by moderate-to-high *TACSTD2* expression, displayed relatively high ORRs to sacituzumab govitecan and datopotamab deruxtecan. However, this trend was inconsistent across histologies.

Finally, to explore potential mechanisms underlying treatment-related toxicities, we compared the expression levels of these genes in normal tissues with the distribution of adverse events (AEs) observed in anti-Trop2 ADC monotherapy trials (Fig. 5b). No direct quantitative correlation emerged, yet tissues with relatively high expression of lysosomal proteases (*CTSB, CTSL*) and *TOP1*, such as gastrointestinal and salivary gland epithelia, overlapped with those most frequently affected by grade ≥3 AEs. In contrast, hematologic AEs such as neutropenia did not align with expression patterns, consistent with the very low levels of *TACSTD2* and ADC-processing gene expression in bone marrow.

Discussion

Our pan-cancer, multi-omic analysis shows that *TACSTD2* (Trop2) expression predominantly occurs in epithelial cells and is enriched in multiple epithelial malignancies (notably breast, cervical, bladder, pancreatic, prostate and lung). It is largely absent from mesenchymal and central nervous system tumors. This epithelial restriction, confirmed at single-cell resolution, supports Trop2 as a relevant yet tissue-specific therapeutic antigen. However, Trop2 is also expressed in several normal epithelia (e.g., salivary gland, gastrointestinal and respiratory epithelia). This highlights the need for careful consideration when predicting on-target/off-tumor toxicity and patient selection.

Single-cell data localize *TACSTD2* expression to specific epithelial lineages (e.g., basal respiratory cells, keratinocytes, ductal cells). This finding reinforces the idea that Trop2 reflects epithelial differentiation programs rather than being a generic "tumor" marker. This biological specificity both explains the therapeutic opportunity and the constraints imposed by normal-tissue expression.

At the molecular level, *TACSTD2* shows few recurrent mutations or copy-number events. Instead, DNA methylation is inversely associated with expression in many cancers, implicating epigenetic control as the dominant regulatory axis. This suggests that epigenetic regulation could be a therapeutic target. ADC efficacy often depends on target expression levels, so strategies to increase *TACSTD2* expression could enhance treatment responsiveness, particularly in cancers with low baseline expression, and especially in tumor types where a relationship between Trop2 levels and therapeutic efficacy has been clinically observed. This aligns with prior preclinical studies showing that treatment with DNA-demethylating agents, such as 5-azacytidine and decitabine, can restore *TACSTD2* expression[24] and synergize with SG[25]. However, the available data remain preclinical and require prospective clinical evaluation before this strategy can be considered in practice.

We also observed tumor-specific associations between *TACSTD2* and common driver alterations, indicating that oncogenic signaling may shape Trop2 programs in a context-dependent manner. For example, in papillary thyroid carcinoma (THCA), tumors with *BRAF* mutations showed significantly higher *TACSTD2* levels, while those with *NRAS* mutations had reduced expression compared to wild-type samples. Interestingly, this finding may help contextualize the heterogeneous methylation pattern observed in THCA, which likely reflects molecular heterogeneity within thyroid tumors driven by different oncogenic mutations. BRAF mutation may be an important factor influencing *TACSTD2* expression, directly or indirectly promoting *ERK* pathway activation and leading to tumorigenesis[26]. The interplay between somatic alterations and *TACSTD2* expression appears to be tumor-specific, with potential implications for disease stratification and combination therapy development, though further research is needed.

Pathway analyses across cancer types showed that *TACSTD2* expression strongly correlates with epithelial differentiation and organization, particularly through claudin family members (CLDN7, CLDN4, CLDN1). This finding is consistent with previous research indicating that Trop2 modulates epithelial barrier integrity via claudin-7 interactions, thereby influencing immune cell access to tumor tissue[27]. Loss of Trop2 disrupts junctional integrity, enhances immune infiltration, and has been associated with improved responses to immune-checkpoint blockade in preclinical TNBC models[27]. However, in our analysis, associations with immune-related pathways were heterogeneous and lacked a consistent pan-cancer enrichment pattern. In some tumor types, such as THCA and KICH, *TACSTD2* expression was positively associated with increased immune cell infiltration, whereas in others, including KIRC and CHOL, it was linked to stromal enrichment and limited cytotoxic immune infiltration, consistent with immune exclusion. This context-dependent pattern is consistent with prior clinical and preclinical observations across tumor types. While Trop2 positivity correlates with higher $CD8^+$ infiltration and PD-L1 expression in cervical cancer[28], it associates with immune exclusion and checkpoint-inhibitor resistance in NSCLC[29,30] and TNBC[30]. This divergence suggests that Trop2 role in immune regulation is not uniform, but instead reflects the integration of epithelial architecture with microenvironmental signals in a tumor-type-specific manner. Accordingly, Trop2 expression may be better interpreted as a marker of epithelial state that indirectly shapes immune accessibility, rather than a direct indicator of immune activation. Translating this biology into the clinic, trials combining Trop2-directed ADCs with immune-checkpoint inhibitors have reported encouraging activity across breast, lung, and other epithelial malignancies.

Correlations between TACSTD2 and putative ADC-processing genes (CTSB, CTSL, TOP1) were modest and variable by histology, underscoring that basal transcript levels of a few genes are insufficient to predict ADC efficacy or toxicity. ADC performance reflects a multi-step process (antigen density, internalization, linker cleavage, payload sensitivity, TME effects) and will likely require composite, function-oriented biomarkers rather than single-gene surrogates.

Despite being both topoisomerase I (TOP1) inhibitors, the payloads SN-38 (the active metabolite of irinotecan, used in SG) and DXd (used in Dato-DXd and the anti-Her2 trastuzumab-deruxtecan [T-DXd]) differ significantly in potency, linker chemistry, drug-to-antibody ratio (DAR), membrane permeability, and bystander killing mechanisms. All these aspects translate into distinct pharmacologic and clinical profiles[31]. DXd achieves cytotoxicity at substantially lower concentrations and shows a more potent bystander effect. SG uses a pH-sensitive hydrolyzable linker that undergoes more rapid hydrolysis intracellularly, while the T-DXd linker is highly stable in plasma and selectively cleaved by lysosomal cathepsins upregulated in tumor cells. Consistently, the activity of action of T-DXd, depends both on HER2 expression levels and extracellular cathepsins[32]. Moreover, protease activity is dynamic and regulated post-transcriptionally. Therefore, protease mRNA alone is an unreliable proxy for extracellular/intracellular cleavage capacity[33]. Functional assays or spatial proteomics may better capture the relevant biology.

In short, anti-Trop2 ADC response is multifactorial: antigen abundance matters, but so do epigenetic state, processing capacity, subcellular localization and the TME[34].

From a translational perspective, the current reliance on IHC-based assessment introduces significant uncertainty in interpreting clinical data. Most pivotal trials, including ASCENT, used semi-quantitative H-scores, yet recent studies have demonstrated considerable inter-assay variability among anti-Trop2 antibodies and only moderate concordance across platforms[35]. Moreover, subcellular localization of Trop2 may be more informative than overall expression levels for predicting ADC efficacy and toxicity. Emerging analyses suggest that membrane-localized Trop2, rather than diffuse or predominantly cytoplasmic staining, may correlate more closely with response to Trop2-directed ADCs, consistent with the biological requirement for surface antigen accessibility to enable antibody binding and payload delivery[36,37].

Recent computational pathology approaches have refined Trop2 quantification through continuous AI-assisted metrics that specifically capture membrane localization, such as the Normalized Membrane Ratio (NMR) or Quantitative Continuous Scoring (QCS-NMR).

In exploratory analyses of the TROPION-Lung01 trial, patients with higher membrane-localized Trop2 scores were more likely to respond to Dato-DXd, supporting the potential predictive value of membrane-specific quantification beyond conventional IHC H-scores[38,39]. These findings underscore the need for standardized, quantitative assays that integrate spatial and subcellular information. In parallel, the emerging field of Trop2 theranostics may provide a more reliable framework for patient selection. Novel agents, including ^68Ga-NOTA-T4 immunoPET[40], ^64Cu/^177Lu-hIMB1636[41], and ^89Zr/^177Lu-NY003[42], shown great potential in quantifying Trop2 expression in-vivo and in delivering targeted radioimmunotherapy. These tools may bridge the gap between diagnostics and therapeutics, supporting a personalized approach to ADC deployment.

Future research priorities are: (1) prospective correlative studies embedding standardized, quantitative Trop2 assays (membrane metrics, immunoPET) into ADC trials; (2) functional readouts of ADC-processing

(activity assays, spatial proteomics); (3) mechanistic evaluation of epigenetic priming in rigorously designed early-phase trials; and (4) longitudinal sampling to capture antigen dynamics and acquired resistance.

Despite its comprehensiveness, our study has several limitations, primarily related to data characteristics and analytical approaches. First, bulk RNA sequencing limits our ability to detect cell-specific expression patterns, though single-cell analyses have partially addressed this issue. However, single-cell data introduce other limitations, including sampling biases and potential loss of cellular context. Second, the observational nature of TCGA and GTEx datasets inherently limits causal interpretations, requiring careful extrapolation to clinical settings without additional experimental validation. Moreover, these datasets lack detailed clinical follow-up information, limiting the depth of prognostic assessments. Third, the infrequency of genetic alterations involving Trop2 prevented an in-depth investigation into mutation-driven mechanisms affecting its expression, constraining comprehensive genomic characterization. Finally, the absence of direct experimental validation for proposed epigenetic strategies (e.g., demethylating agents) requires cautious interpretation of their clinical relevance until supported by confirmatory studies.

In conclusion, our integrative, pan-cancer analysis delineates Trop2 as an epithelial-restricted antigen whose therapeutic relevance for ADCs extends beyond target abundance. Epigenetic regulation, membrane localization, and tumor-intrinsic processing capacity collectively shape Trop2 expression and its therapeutic window across malignancies. These findings highlight the need for standardized, quantitative assays to refine patient selection and interpret ADC activity more accurately. Incorporating multiomic and functional biomarkers into future clinical trials will be essential to capture antigen dynamics, anticipate resistance, and guide rational combination strategies, including epigenetic priming and immunomodulation. Through such integrated, prospective efforts, Trop2 targeting can be optimized across tumor types while minimizing the risk of toxicities.

Methods

Data sources

To avoid technical bias between different datasets, we obtained uniformly re-processed bulk RNA-Seq transcript per million (TPM) data and sample annotations for The Cancer Genome Atlas (TCGA) and the Genotype-Tissue Expression (GTEx) using the recount3 Bioconductor package[43]. All other TCGA pan-cancer data types, clinical annotations, somatic mutations, somatic copy-number aberrations, and Illumina 450k Methylation beta value data were downloaded using the TCGABiolinks package[44]. The number of available samples by tissue and data type is reported in Table S1. Pan-cancer TCGA survival data were downloaded were obtained from the TCGA-Clinical Data Resource[45]. For tumor single-cell RNA-Seq analysis, we queried for *TACSTD2* expression in the Curated Cancer Cell Atlas[46]. Only solid tumors were included in the analysis; hematologic malignancies were excluded. For normal tissues, single-cell RNA-Seq data were retrieved from the Human Protein Atlas database[47].

For the analysis of clinical efficacy of anti-Trop2 ADCs, trial-reported objective response rates (ORRs) from monotherapy studies/cohorts were extracted from publicly available phase I/II/III clinical trials (Table S2). We selected ORR for cross-trial comparison because it was the most consistently reported efficacy endpoint across available monotherapy ADC studies, particularly in early-phase settings, and is less susceptible than progression-free survival to biases related to assessment timing or composite event definitions. For the toxicity analysis, any grade and grade ≥3 adverse event (AE) frequencies were retrieved from the same trials and matched to corresponding normal tissues according to established organ-toxicity relationships (e.g., gastrointestinal epithelium-diarrhea; salivary gland/oral mucosae-mucositis; skin-rash). The correspondence between AE categories and GTEx tissues is detailed in Table S3. All clinical data (ORRs and AEs) were last accessed and downloaded from public sources on June 27, 2024.

Statistical analysis

TPM values of TCGA and GTEx RNA-Seq data were log2-transformed after adding a constant value of 1 to avoid infinite values. For downstream analyses, only TCGA samples annotated as "Primary tumor" were selected. In GTEx, samples with missing tissue annotation were discarded. To define samples with high expression of *TACSTD2* we pooled all healthy tissue data from GTEx, and we identified the threshold corresponding to the 80th percentile of the distribution of *TACSTD2* $\log_2$(TPM) expression values. Individual samples with an expression value above this cut-off were considered high *TACSTD2* expressors. This approach was selected to identify tumor samples with expression levels exceeding the physiological range observed in the majority of normal tissues, thereby providing a biologically informed and pan-cancer–consistent definition of relative overexpression. For downstream genomic analyses only cancer types with at least 10% of samples with high *TACSTD2* expression were selected.

For somatic mutations analysis, we discarded synonymous mutations and considered only those with high or moderate variant consequences according to the Ensembl classification[48]. In addition, we further selected only somatic mutations with validated oncogenic status according to the Cancer Genome Interpreter database[49].

For somatic copy-number aberrations, absolute copy-number values were downloaded. A gene was considered deleted if its absolute copy-number value was equal to 0. To call a gene amplified, we considered an absolute copy number cut-off greater than 6. Only genes with known oncogenic or oncosuppressor function were considered, according to the Cancer Genome Interpreter database[49].

Association between continuous *TACSTD2* expression and binary categorical variables such as sex (male vs female) and mutational status (mutant versus wild-type) was performed using an unpaired two-tailed Student's *t* test. Association between continuous *TACSTD2* expression and multiple categorical variables, such as age (10-years intervals groups) and somatic copy number status (deleted, normal, amplified), was performed using ANOVA.

Correlation between *TACSTD2* expression and somatic copy number values, methylation status, and CTSB, CTSL, and TOP1 gene expression values was performed using the Spearman correlation coefficient.

To estimate the relative abundance of immune and stromal cell populations across tumor samples, we applied the consensusTME (cTME) framework[50], which integrates multiple tumor-type–specific gene signatures optimized for robust deconvolution in bulk RNA-seq data.

We evaluated pathway activity using the Hallmark gene sets from the Molecular Signatures Database[43]. To assess the association between TACSTD2 expression and pathways and cTME cell types, we employed a linear modeling approach using the LIMMA package[51]. For each tumor type, singscore-derived pathway activity scores were modeled as a function of TACSTD2 expression treated as a continuous variable. The resulting regression coefficient represents the direction and magnitude of the association between TACSTD2 expression and pathway activity. Multiple testing correction of p-values was performed using the Benjamini-Hochberg false discovery rate (FDR) method. To estimate pathway activity at the single-sample level, we applied the singscore method[52],a rank-based, non-parametric approach that assigns enrichment scores independently for each sample.

Survival analysis for continuous *TACSTD2* expression in each cancer type was performed using the Cox-proportional hazard model. For visualization, the Kaplan-Meier curves method with log-rank test for p-value calculation was employed, using the median *TACSTD2* expression value as cut-off for variable dichotomization.

Ethical approval

This study used de-identified, publicly available data and did not require institutional review board approval.

Data availability

All data analyzed in this study are publicly available from the following sources:- The Cancer Genome Atlas (TCGA) via the Genomic Data Commons (https://portal.gdc.cancer.gov/),- Genotype-Tissue Expression (GTEx) project (https://gtexportal.org/home/),- Single-cell transcriptomic datasets from publicly available atlases, including the Human Protein Atlas (https://www.proteinatlas.org/), Human Cell Atlas (https://data.humancellatlas.org/)- Curated data and the R code to reproduce the analyses are available at the following GitHub repository: https://github.com/mdugo/pan-cancer_TROP2.

Received: 3 February 2026; Accepted: 15 May 2026;
Published online: 15 June 2026

References

1. Lombardi, P. et al. Overview of trop-2 in cancer: from pre-clinical studies to future directions in clinical settings. *Cancers* https://doi.org/10.3390/cancers15061744 (2023).
2. Lipinski M., Parks D. R., Rouse R. V., Herzenberg L. A. *Human Trophoblast Cell-Surface Antigens Defined by Monoclonal Antibodies (Choriocarcinoma/Fetal Cells/Fluorescence-Activated Cell-Sorter)*. Vol 78. https://www.pnas.org (1981).
3. Zaman, S., Jadid, H., Denson, A. C. & Gray, J. E. Targeting Trop-2 in solid tumors: future prospects. *Onco Targets Ther.* **12**, 1781–1790 (2019).
4. Shvartsur A., Bonavida B. *Trop2 and Its Overexpression in Cancers: Regulation and Clinical/ Therapeutic Implications*. Vol 6. www.impactjournals.com/Genes&Cancer (2015).
5. Stepan, L. P. et al. Expression of Trop2 cell surface glycoprotein in normal and tumor tissues: potential implications as a cancer therapeutic target. *J. Histochem. Cytochem.* **59**, 701–710 (2011).
6. Bosi, C. et al. Pan-cancer analysis of antibody-drug conjugate targets and putative predictors of treatment response. *Eur. J. Cancer* https://doi.org/10.1016/j.ejca.2023.113379 (2023).
7. Trerotola, M. et al. Upregulation of Trop-2 quantitatively stimulates human cancer growth. *Oncogene* **32**, 222–233 (2013).
8. Zeng, P. et al. Impact of TROP2 expression on prognosis in solid tumors: a systematic review and meta-analysis. *Sci. Rep. Nat. Publ. Group.* https://doi.org/10.1038/srep33658 (2016).
9. Syed, Y. Y. Sacituzumab Govitecan: first approval. *Drugs* **80**, 1019–1025 (2020).
10. Rugo, H. S. et al. Overall survival with sacituzumab govitecan in hormone receptor-positive and human epidermal growth factor receptor 2-negative metastatic breast cancer (TROPiCS-02): a randomised, open-label, multicentre, phase 3 trial. *Lancet.* **402**, 1423–1433 (2023).
11. Okajima, D. et al. Datopotamab deruxtecan, a novel TROP2-directed antibody-drug conjugate, demonstrates potent antitumor activity by efficient drug delivery to tumor cells. *Mol. Cancer Ther.* **20**, 2329–2340 (2021).
12. Han, C. et al. In vitro and in vivo activity of sacituzumab govitecan, an antibody-drug conjugate targeting trophoblast cell-surface antigen 2 (Trop-2) in uterine serous carcinoma. *Gynecol. Oncol.* **156**, 430–438 (2020).
13. Perrone, E. et al. Sacituzumab govitecan, an antibody-drug conjugate targeting trophoblast cell-surface antigen 2, shows cytotoxic activity against poorly differentiated endometrial adenocarcinomas in vitro and in vivo. *Mol. Oncol.* **14**, 645–656 (2020).
14. Perrone, E. et al. Preclinical activity of sacituzumab govitecan, an antibody-drug conjugate targeting trophoblast cell-surface antigen 2 (Trop-2) linked to the active metabolite of irinotecan (SN-38), in ovarian cancer. *Front. Oncol.* https://doi.org/10.3389/fonc.2020.00118 (2020).
15. Loriot, Y. et al. Sacituzumab govitecan demonstrates efficacy across tumor Trop-2 expression levels in patients with advanced urothelial cancer. *Clin. Cancer Res.* **30**, 3179–3188 (2024).
16. Bardia, A. et al. Biomarker analyses in the phase III ASCENT study of sacituzumab govitecan versus chemotherapy in patients with metastatic triple-negative breast cancer. *Ann. Oncol.* **32**, 1148–1156 (2021).
17. Coates, J. T. et al. Parallel genomic alterations of antigen and payload targets mediate polyclonal acquired clinical resistance to sacituzumab govitecan in triple-negative breast cancer. *Cancer Discov.* **11**, 2436–2445 (2021).
18. Ajkunic, A. et al. Assessment of TROP2, CEACAM5 and DLL3 in metastatic prostate cancer: expression landscape and molecular correlates. *npj Precis. Oncol.* https://doi.org/10.1038/s41698-024-00599-6 (2024).
19. Morgenstern-Kaplan D., et al. Genomic, immunologic, and prognostic associations of TROP2 (TACSTD2) expression in solid tumors. *Oncologist*. Published online. https://doi.org/10.1093/oncolo/oyae168 (2024).
20. Tsui, C. K. et al. CRISPR-Cas9 screens identify regulators of antibody-drug conjugate toxicity. *Nat. Chem. Biol.* **15**, 949–958 (2019).
21. Colombo, R., Tarantino, P., Rich, J. R., Lorusso, P. M. & de Vries, E. G. E. The journey of antibody-drug conjugates: lessons learned from 40 years of development. *Cancer Discov.* **14**, 2089–2108 (2024).
22. Coorens, T. H. H. et al. The human and non-human primate developmental GTEx projects. *Nature* **637**, 557–564 (2025).
23. Tomczak K., Czerwińska P., Wiznerowicz M. The Cancer Genome Atlas (TCGA): an immeasurable source of knowledge. *Contem. Oncol*. **2015**, 68–77 (2015)
24. Gehring, A. et al. DNA demethylation and tri-methylation of H3K4 at the TACSTD2 promoter are complementary players for TROP2 regulation in colorectal cancer cells. *Sci. Rep.* https://doi.org/10.1038/S41598-024-52437-1 (2024).
25. Zhao, M. et al. Epigenetically upregulating TROP2 and SLFN11 enhances therapeutic efficacy of TROP2 antibody drug conjugate sacitizumab govitecan. *npj Breast Cancer* https://doi.org/10.1038/S41523-023-00573-8 (2023).
26. Kong, J. S. et al. The significance of TROP2 expression in predicting BRAF mutations in papillary thyroid carcinoma. *J. Pathol. Transl. Med.* **52**, 14–20 (2018).
27. Yin, Q. et al. Navigating the future of gastric cancer treatment: a review on the impact of antibody-drug conjugates. *Cell Death Discov.* **11**, 144 (2025).
28. Chiba, Y. et al. Trop-2 expression and the tumor immune microenvironment in cervical cancer. *Gynecol. Oncol.* **187**, 51–57 (2024).
29. Bessede, A. et al. TROP2 is associated with primary resistance to immune checkpoint inhibition in patients with advanced non-small cell lung cancer. *Clin. Cancer Res.* **30**, 779–785 (2024).
30. Wu, B. et al. TROP2/claudin program mediates immune exclusion to impede checkpoint blockade in breast cancer. *J. Immunother. Cancer* **14**, e012265 (2026).
31. Yao, B. et al. Selection of payloads for antibody-drug conjugates targeting ubiquitously expressed tumor-associated antigens: a case study. *AAPS J.* https://doi.org/10.1208/s12248-022-00720-2 (2022).
32. Tsao, L. C. et al. Effective extracellular payload release and immunomodulatory interactions govern the therapeutic effect of trastuzumab deruxtecan (T-DXd). *Nat. Commun.* https://doi.org/10.1038/s41467-025-58266-8 (2025).
33. Jakoš, T., Pišlar, A., Jewett, A. & Kos, J. Cysteine cathepsins in tumor-associated immune cells. *Front. Immunol.* https://doi.org/10.3389/fimmu.2019.02037 (2019).
34. Vogel, M., Colombo, R. & Tarantino P. Beyond the guided missile paradigm: embracing the complexity of antibody-drug conjugates. *J. Clin. Oncol*. https://doi.org/10.1200/JCO-25-01235 (2025).

35. Cursano, G. et al. Inter-assay variability of TROP2 immunohistochemistry in triple-negative breast cancer. *Mol. Diagn Ther*. https://doi.org/10.1007/S40291-025-00814-5/FIGURES/3 (2025).
36. Sung, M. S. et al. Abstract 7149: the role of TROP2 in the MoA of Dato-DXd and how it underpins the biologic rationale of the novel AI-guided biomarker TROP2 normalized membrane ratio. *Cancer Res.* **85**, 7149–7149 (2025).
37. Meric-Bernstam, F. et al. Antitumor activity and biomarker analysis for TROP2 antibody–drug conjugate datopotamab deruxtecan in patient-derived breast cancer xenograft models. *Clin. Cancer Res.* **31**, 573 (2024).
38. Garassino, M. C. et al. PL02.11 normalized membrane ratio of TROP2 by quantitative continuous scoring is predictive of clinical outcomes in TROPION-Lung 01. *J. Thorac. Oncol.* **19**, S2–S3 (2024).
39. Wu, Y. L. et al. 357P: Association of TROP2 quantitative continuous scoring (QCS) normalised membrane ratio (NMR) with efficacy in Chinese patients (pts) with advanced/metastatic non-small cell lung cancer (a/mNSCLC) treated with datopotamab deruxtecan (Dato-DXd) in TROPION-PanTumor02. *J. Thorac. Oncol.* **20**, S212–S213 (2025).
40. Jiang, D. et al. [68Ga]Ga-NOTA-T4 ImmunoPET imaging for evaluating TROP2 expression in patients with solid tumors. *Eur. J. Nucl. Med. Mol. Imaging*. https://doi.org/10.1007/s00259-025-07326-8 (2025).
41. Li, C. et al. Theranostic application of 64Cu/177Lu-labeled anti-Trop2 monoclonal antibody in pancreatic cancer tumor models. *Eur. J. Nucl. Med Mol. Imaging* **50**, 168–183 (2022).
42. Wu, Y. et al. Preclinical evaluation of the theranostic potential of 89Zr/177Lu-labeled anti-TROP-2 antibody in triple-negative breast cancer model. *EJNMMI Radiopharm. Chem.* **9**, 5 (2024).
43. Liberzon, A. et al. Molecular signatures database (MSigDB) 3.0. *Bioinformatics* **27**, 1739–1740 (2011).
44. Colaprico, A. et al. TCGAbiolinks: an R/bioconductor package for integrative analysis of TCGA data. *Nucleic Acids Res.* **44**, e71 (2016).
45. Liu, J. et al. An integrated TCGA pan-cancer clinical data resource to drive high-quality survival outcome analytics. *Cell* **173**, 400–416.e11 (2018).
46. Tyler, M. et al. The curated cancer cell Atlas provides a comprehensive characterization of tumors at single-cell resolution. *Nat Cancer*. https://doi.org/10.1038/s43018-025-00957-8 (2025).
47. Karlsson, M. et al. A single-cell type transcriptomics map of human tissues. *Sci. Adv*. https://doi.org/10.1126/sciadv.abh2169 (2021).
48. Dyer, S. C. et al. Ensembl 2025. *Nucleic Acids Res.* **53**, D948–D957 (2025).
49. Tamborero, D. et al. Cancer Genome Interpreter annotates the biological and clinical relevance of tumor alterations. *Genome Med.* **10**, 25 (2018).
50. Jimenez-Sanchez, A., Cast, O. & Miller, M. L. Comprehensive benchmarking and integration of tumor microenvironment cell estimation methods. *Cancer Res.* **79**, 6238–6246 (2019).
51. Ritchie, M. E. et al. limma powers differential expression analyses for RNA-sequencing and microarray studies. *Nucleic Acids Res.* **43**, e47 (2015).
52. Foroutan, M. et al. Single sample scoring of molecular phenotypes. *BMC Bioinform.* https://doi.org/10.1186/s12859-018-2435-4 (2018).

Acknowledgements

This study was supported by Gilead through the grant for data publication "Espressione e significato clinico-biologico di TROP2 nel pancancer" (2022–2023). The funders had no role in study design, data collection, analysis, interpretation of data, or in writing the manuscript.GB is also supported by a donation from Carmelina Ratto and Carlo Capra. CB is supported by an American-Italian Cancer Foundation Post-Doctoral Research Fellowship (2024–2025).

Author contributions

G.B. led the conception and design of the study and supervised the project. G.N., B.G., G.V., M.D., M.M.N., and C.B. contributed to the conception and design of the study. G.N., B.G., G.V., and M.D. wrote the original draft of the manuscript. B.G., and M.D. performed the statistical and bioinformatic analyses and prepared the figures. G.D.M, L.L., M.M., M.P., C.C., M.B., M.C., C.Z., F.P., A.C., J.M.P.G., H.R.A., J.C., and L.P. contributed to data interpretation and provided critical intellectual input. All the authors (G.N, B.G., M.M.N., C.B., G.D.M., L.L., M.M., M.P., C.C., M.B., M.C.,C.Z., F.P., A.C., J.M.P.G., H.R.A., J.C., L.P., L.G., G.B., and M.D.) critically revised the manuscript, and approved the final version.

Competing interests

GN reports travel, accommodation, and expenses for scientific meetings from Eli Lilly, Sanofi, and MSD. GV reports support for travel from Eli Lilly, Pfizer, and AstraZeneca; advisory board participation for Pfizer and Novartis; and speaker fees from Daiichi Sankyo and Eli Lilly. MMN reports travel, accommodation, and expenses for scientific meetings from Eli Lilly and Daiichi Sankyo. CB reports grants from the American-Italian Cancer Foundation during the conduct of the study, as well as other support from Gilead Sciences, Daiichi Sankyo, and Eli Lilly and Company, and personal fees from MSD outside the submitted work. LL reports personal fees for consultancy, advisory board participation, and speaker bureau activities from AstraZeneca, Daiichi Sankyo, Eli Lilly, Novartis, Pfizer, Gilead, Exact Sciences, Helsinn, Roche, Italfarmaco, Accord, Eisai, and Takeda; and support for attending meetings from Gilead, Accord, Helsinn, Roche, and Daiichi Sankyo. MM reports travel grants from Gilead and Eli Lilly. MP reports travel, accommodation, and expenses from Novartis and Eli Lilly. CC reports consultancy, advisory roles, and speaker bureau participation for Pfizer, Novartis, Eli Lilly, Roche, MSD, Daiichi Sankyo, AstraZeneca, Gilead, and Menarini Stemline. CZ reports travel, accommodation, and expenses for scientific meetings from Gilead. FP reports support for attending meetings from Menarini, Gilead, Pfizer, and Eli Lilly. AC reports support for attending meetings from Pfizer, Eli Lilly, and Novartis. JP reports advisory roles for Eli Lilly, Roche, Eisai, MSD, Daiichi Sankyo, AstraZeneca, Seattle Genetics, and Gilead; and travel expenses from Roche and Daiichi Sankyo. JC reports consultancy, advisory board participation, and honoraria from Roche, AstraZeneca, Daiichi Sankyo, Eli Lilly, Novartis, Pfizer, Merck Sharp & Dohme, Gilead, Eisai, Seattle Genetics, Menarini, Boehringer Ingelheim, Clovis Oncology, Jazz Pharmaceuticals, AbbVie, BioNTech, Zymeworks, Biocon, Circle Pharma, Delcath Systems, Hexagon Bio, Hibercell, BioInvent, Gemoab, Leuko, Bioasis, Ellipses, Reveal Genomics, Scorpion Therapeutics, Expres2ion Biotechnologies, BridgeBio, Bliss Biopharmaceutical, Stemline Therapeutics, and Zuellig Pharma.Research funding to the institution has been received from Roche, F. Hoffmann–La Roche, AstraZeneca, Ariad Pharmaceuticals, Baxalta GmbH/Servier Affaires, Bayer Healthcare, Eisai, Guardant Health, Merck Sharp & Dohme, Pfizer, Piqur Therapeutics, IQVIA, and Queen Mary University of London.Support for travel, accommodation, and meeting expenses has been received from Roche, Novartis, Eisai, Pfizer, Daiichi Sankyo, AstraZeneca, Gilead, Merck Sharp & Dohme, and Stemline Therapeutics.Stock ownership is reported in MAJ3 Capital and Leuko (relative).JC is a co-inventor on patents related to pharmaceutical combinations of a PI3K inhibitor and a microtubule-destabilizing agent (WO 2014/199294 A; issued) and HER2 as a predictor of response to dual HER2 blockade in the absence of cytotoxic therapy (US 2019/0338368 A1; licensed). LP reports consultancy, advisory board participation, and honoraria from Merck & Co., AstraZeneca, Bristol Myers Squibb, Agendia, Radionetics, Natera, and Personalis. Research funding to the institution has been received from Merck & Co., AstraZeneca, Bristol Myers Squibb, Pfizer, Menarini, Natera, Exact Sciences, Personalis, and Agendia. Stock ownership is reported in Ataraxis. LG reports advisory board participation and consultancy for AstraZeneca, Roche, Synaffix, Zymeworks, Daiichi Sankyo, BeiGene, Revolution Medicines, Menarini Ricerche, and Denali Therapeutics Inc; and is a co-inventor of European Patent Applications No. 12195182.6 and 12196177.5 titled "PD-L1 expression in anti-HER2 therapy" (Roche; no compensation provided). GB reports personal fees for consultancy, honoraria, and advisory

roles from AstraZeneca, Daiichi Sankyo, Eli Lilly, Novartis, Pfizer, Roche, MSD, Gilead, Menarini, Exact Sciences, Seagen, Helsinn, Takeda, and Amgen. MD reports travel expenses from Insight Molecular Diagnostics. The other authors declare no competing financial or non-financial interests.

Additional information

Supplementary information The online version contains supplementary material available at https://doi.org/10.1038/s41698-026-01523-w.

Correspondence and requests for materials should be addressed to Giampaolo Bianchini.